

COSMIC RAY ELEMENTAL ABUNDANCES FOR  $26 \leq Z \leq 40$  MEASURED ON HEAO-3T. L. Garrard<sup>1</sup>, M. H. Israel<sup>2</sup>, J. Klarmann<sup>2</sup>, E. C. Stone<sup>1</sup>, C. J. Waddington<sup>3</sup>, and W. R. Binns<sup>2</sup>

1) California Institute of Technology, Pasadena, California 91125 USA

2) Washington University, St. Louis, Missouri 63130

3) University of Minnesota, Minneapolis, Minnesota 55455 USA

**Abstract**

Abundances relative to  ${}^{26}\text{Fe}$  have been derived for elements with charge,  $Z$ , in the range  $32 \leq Z \leq 40$ . With a resolution better than 0.5 charge unit at  $Z=38$ , we resolve  ${}^{37}\text{Rb}$  from  ${}^{38}\text{Sr}$  and use the Rb/Sr ratio to place a limit on the r-process enhancement of the cosmic ray source material in this charge range.

**Introduction:** We have derived elemental abundances of ultraheavy elements ( $Z > 30$ ) relative to Fe using the data from the HEAO-3 Heavy Nuclei Experiment, the HNE, Binns *et al.* 1981b. The data were selected for the best charge resolution available, consistent with retaining statistical significance for the relatively abundant ultraheavy elements with  $Z < 42$ . This analysis has the purpose of providing the best possible abundances for the odd elements, especially  ${}^{37}\text{Rb}$  which is an r-process indicator. Incremental improvements in charge assignment and analysis techniques since our previous analyses of data in this charge range (Binns *et al.* 1981a; 1983) yield a more convincing upper limit on the r-process component of the cosmic radiation.

**Instrument; Data Selection:** The HNE instrument was used to determine charge and energy of ultraheavy nuclei based on ionization energy loss (in charge units, the signal  $\propto Z_1^2$ ), Cherenkov light ( $\propto Z_C^2$ ), and geomagnetic cutoff rigidity ( $R_C$ ). The current results are based on two data sets: The first -- the high  $R_C$  data set -- includes all nuclei observed at  $R_C > 8.8$  GV, which corresponds to 3.27 GeV/nuc for  ${}^{56}\text{Fe}$  ( $\sim 3.0$  for  ${}^{38}\text{Sr}$ ). The second -- the low energy (E) data set -- includes all nuclei with  $0.33 \leq Z_C/Z_1 \leq 0.82$ , roughly 340 MeV/nuc to 950 MeV/nuc. In order to guarantee the accuracy of the charge measurement and improve the resolution, both data sets are subjected to internal consistency requirements. The most important of these is the requirement that  $Z_1$  be measured and consistent on both sides of the Cherenkov counter.

**Analysis:** In order to deconvolve the charge spectrum from the measured distribution of signals it is necessary to take account of the resolution function of the instrument. In the high  $R_C$  data set, the spreading due to energy dispersion is small enough that photoelectron statistics and mapping errors dominate; hence the resolution function is expected to be Gaussian. Here again, we have improved resolution at the cost of statistical significance. In the low E data set the resolution function is well-approximated by a Gaussian as can be seen for the Fe peak, see Figure 1.

We have assumed Gaussian resolution functions and allowed the width to vary linearly with charge. Using maximum likelihood techniques, the best fits to the summed data set are obtained with a resolution of  $\sigma = 0.32$  charge units at Fe and  $\sigma = 0.47 \pm 0.06$  charge units at Sr. The offsets of the peaks from the integer values ( $\Delta$ ) are not significant; the best fit values show the Fe peak at  $Z = 26.015 \pm 0.010$  and the Sr peak at  $Z = 38.14 \pm 0.07$ . With these fit parameters, the low E data set corresponds to 0.742 million Fe events; the high  $R_C$  to 0.772 million; and the summed to 1.52 million.

These fitted abundances are corrected for charge-changing nuclear interactions in the detector by using a slab propagation program based on our measured cross sections for  ${}^{36}\text{Kr}$  on aluminum at 1.4 GeV/nuc (Binns *et al.* 1987; see also paper OG8.3-13, this

Conference.) The resulting abundances are shown in Table 1. The indicated uncertainties include a "systematic" contribution due to uncertainties in  $\sigma$  and  $\Delta$ , but this term is trivial compared to the statistical contribution. No contributions to the uncertainties due to the (generally small) interaction correction are included.

If  $L_0$  is the value of the likelihood function at its maximum, then the uncertainty of the Rb/Sr abundance ratio is more correctly given by the extreme extent of the contour surface of  $\log(L_0)-1/2$  in the three-dimensional space consisting of  $\sigma$  at Sr,  $\Delta$  at Sr, and the Rb/Sr abundance ratio (Yost 1985). This contouring procedure correctly accounts for the correlation between the fitted Rb and Sr abundances and the correlation with  $\sigma$  and  $\Delta$ . We also included a small contribution to the uncertainty due to the interaction correction procedure, but still omitted any uncertainty due to lack of knowledge of cross sections. The Rb/Sr ratio is  $0.27^{+0.13}_{-0.11}$  in the detector and  $0.24 \pm 0.12$  after correction for interactions.

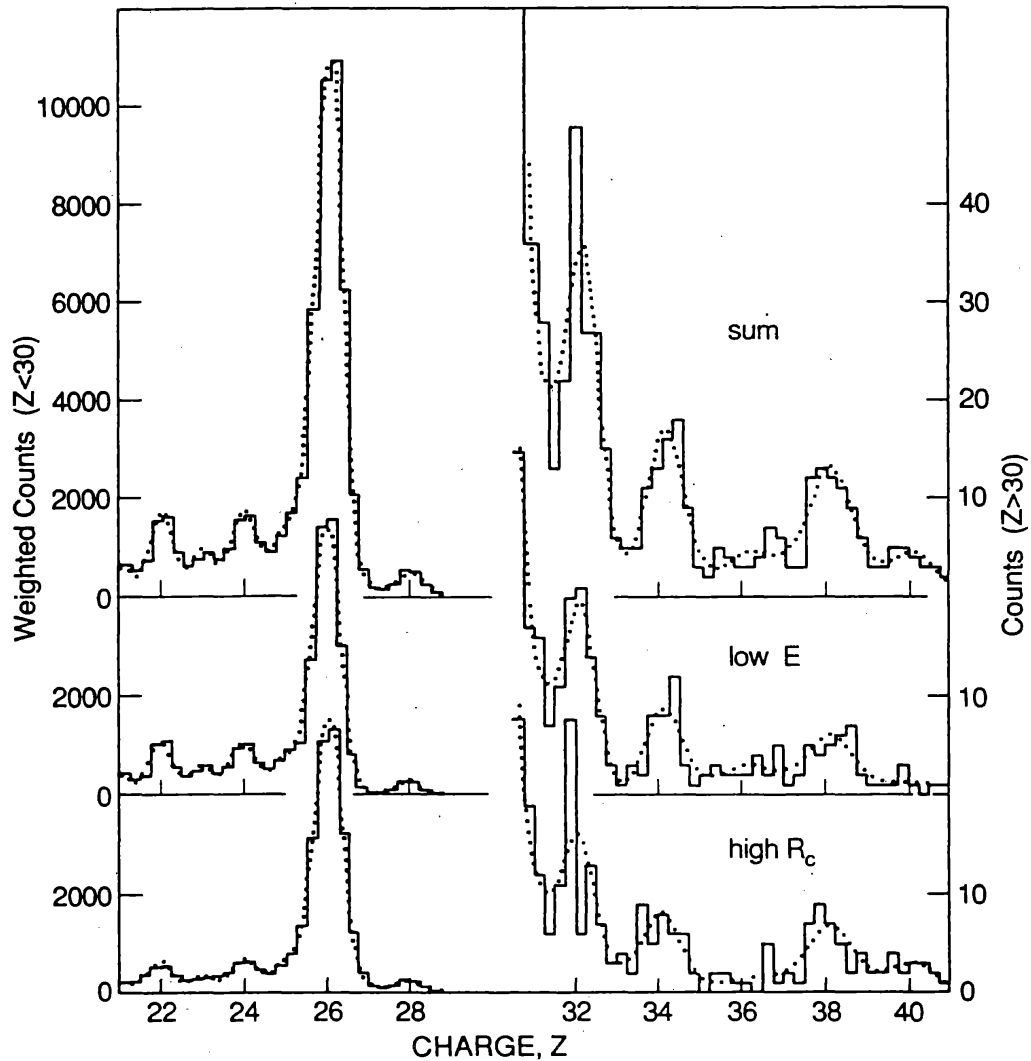


Figure 1: Measured charge histograms and Gaussian fits (dotted lines) for the high  $R_c$ , low  $E$ , and summed data sets. Use the right hand scale for  $Z > 30$ .

**Comparisons:** It is interesting to compare these latest results to our recently published summary data set which was combined with the Ariel-6 data (Fowler *et al.* 1987) to give summary abundance values for ultraheavy galactic cosmic rays (Binns *et al.* 1989). The high  $R_C$  data set is a subset (roughly 10%) of that HNE data set, which included all nuclei with  $Z_C/Z_1 > 0.9$  (i.e.,  $E \gtrsim 1.5$  GeV/nuc). The high  $R_C$  data have a higher minimum energy and a higher average energy than the  $Z_C/Z_1 > 0.9$  data, but energy is not well measured by the HNE above  $\sim 1$  GeV/nuc and the energy distributions of the two data sets are not well known. The low E data set is completely distinct from the other two.

Table 1 also displays a comparison of the current data sets, previous HNE publications, and the Ariel-6 data. The variations in the abundance of  $^{36}\text{Kr}$  among the various data sets are larger than any probable statistical fluctuation. A part of this variation is expected, since Kr is largely secondary and since secondaries are known to be less abundant at high energies. However, the excess Kr at intermediate energies compared to the low E data set, as seen both by us and by Ariel-6, is difficult to explain in terms of the commonly accepted dependence of escape path length on energy (Ormes and Protheroe 1983). We have, of course, closely examined the alternative possibility that the Kr excess is an artifact, due to the poorer resolution observed in the HNE data in this intermediate energy range and in the Ariel-6 data. This alternative appears considerably less plausible; a careful examination of the quality/consistency criteria shows no difference between those events identified as  $Z=36$  compared to  $Z=34$  or  $Z=38$ .

Table 1

Z	low E	high $R_C$	summed	ICRC1983	ApJ1989	Ariel-6
32	107.3±13.5	84.7±12.2	95.5±9.2	91+12,-8		
33	[0.0]±5.1	[9.2]±5.9	[4.0]±3.4	[9]<19	51.2±3.7	66±5
34	50.8±9.2	46.3±9.1	48.5±6.6	43+9,-6		
35	[6.2]±4.9	[4.5]±4.6	[5.3]±3.4	[7]<14	35.1±3.0	39±4
36	16.9±6.7	7.1±5.1	12.0±4.3	23+8,-5		
37	[10.4]±6.2	[9.3]±6.0	9.9±4.4	[9]<16	39.6±3.1	36±4
38	38.7±8.9	42.6±9.2	40.7±6.5	34+10,-6		
39	[5.7]±5.3	[7.5]±5.7	[6.4]±4.0	[5]<12	22.2±2.6	24±4
40	7.3±5.1	19.3±7.3	14.3±4.2	13+5,-4		

We note that a similar possibility of unusual energy dependence was pointed out for the secondaries in the charge region 60 to 74 in Binns *et al.* 1989. However, our marginal statistics and poor energy resolution still do not allow us to claim a clear observation of unusual energy spectra.

Our comparison to models for cosmic ray source abundances and propagation is expressed in terms of two abundance ratios: the  $(^{35}\text{Br} + ^{36}\text{Kr}) / (^{37}\text{Rb} + ^{38}\text{Sr})$  ratio which should be strongly dependent on FIP fractionation effects and only weakly dependent on the nucleosynthesis history of the source material; and the Rb/Sr ratio which is only weakly dependent on FIP but strongly dependent on nucleosynthesis history. Predicted values of these ratios are shown in Figure 2 for a variety of parameters/assumptions:

- source material abundances based on the solar system abundances of Anders and Ebihara (1982), and on the r-/s-process decomposition of Binns *et al.* (1985),
- no fractionation, slant step fractionation (Letaw *et al.* 1984), and exponential FIP fractionation (Brewster *et al.* 1983),
- interaction cross sections based on the semi-empirical fits (Silberberg *et al.* 1985),
- an energy spectrum given by Newport (1986).

Since the present data includes both high  $R_C$  data, with energies somewhat higher than those of Newport and low  $E$  data with energies quite different, additional study will be required to fully characterize this comparison. If the ultraheavy secondaries show the same energy dependence as the secondaries of Fe, then one would predict more Br and Kr at low energies (these elements are nearly 50% secondary at high energies for a solar system source), and some enhancement of Rb (about 15% secondary) at low energies. Until the additional propagation study is complete, the discussion of fractionation must be considered preliminary and qualitative. The r-process/s-process comparison based on the Rb/Sr ratio is less sensitive to this lack.

**Discussion:** It is clear from Figure 2 that the data are not indicative of an r-process source, in agreement with our previous studies of this charge region, and in contrast to the r-process enhancement observed for the  $^{78}\text{Pt}$  group (Binns *et al.* 1989). The low abundance of Kr indicates that some fractionation (presumably FIP related) is necessary; however the Kr abundance of Binns *et al.* (1989) is higher, as noted above. That measurement is consistent with either unfractionated s-process source material or fractionated solar system source material.

The low Rb abundance seen in the current work indicates an enhancement of s-process material in the cosmic ray source. If we assume slant step fractionation, then the Rb/Sr error bars range from pure solar system source to pure s-process source. The s-process source enhancement is qualitatively independent of fractionation model and energy dependence (at the one sigma level).

**Acknowledgements:** This work was supported in part by NASA grants NAG 8-498, 500, and 502; and NGR 05-002-160, 24-005-050, and 26-008-001.

#### References

- Anders and Ebihara 1982 *Geochim. et Cosmochim. Acta* **46**, 2363  
 Binns, Fickle, Garrard, Israel, Klarmann, Stone, and Waddington 1981a *Ap. J. Lett.* **247**, L115  
 Binns, Israel, Klarmann, Scarlett, Stone, and Waddington 1981b *Nucl. Instr. Meth.* **185**, 415  
 Binns, Grossman, Israel, Jones, Klarmann, Garrard, Stone, Fickle, and Waddington 1983 *Proc. 18th Int. Cosmic Ray Conf. (Bangalore)* **9**, 106  
 Binns, Brewster, Fixsen, Garrard, Israel, Klarmann, Newport, Stone, and Waddington 1985 *Ap. J.* **297**, 111  
 Binns, Garrard, Israel, Kertzman, Klarmann, Stone, and Waddington 1987 *Phys. Rev. C* **36**, 1870  
 Binns, Garrard, Gibner, Israel, Kertzman, Klarmann, Newport, Stone, and Waddington 1989 *Ap. J.* **346**, November 15 issue, in press.  
 Brewster, Freier, Waddington 1983 *Ap. J.* **264**, 324  
 Fowler, Walker, Masheder, Moses, Worley, and Gay 1987 *Ap. J.* **314**, 739  
 Newport, B. J. 1986 Ph.D. Thesis, California Institute of Technology  
 Letaw, Silberberg, and Tsao 1984 *Ap. J.* **279**, 144  
 Ormes and Protheroe 1983 *Ap. J.* **272**, 756.  
 Silberberg, Tsao, and Letaw 1985 *Ap. J. Supp.* **58**, 873 and therein.  
 Yost, G. P. 1985 "Lectures on Probability and Statistics", Lawrence Berkeley Lab Report 16993

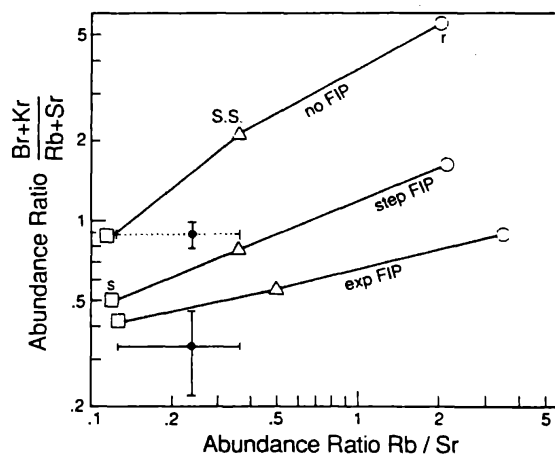


Figure 2: Calculated and measured abundance ratios. This work ●; Binns *et al.* (1989) ● with dotted error bar; s-process □; solar system Δ; r-process ○. For Binns *et al.* (1989) no Rb/Sr ratio was measured and their Rb/Sr co-ordinate and error bar are assumed to be the same as currently measured.